Energy aspects at high power wounded rotor motors startup

Ion Vlad , Sorin Enache, Monica Adela Enache, Ionut D. Smarandescu

***Abstract*—** The actual demand is to optimize the design of the high power three-phase induction motors with wounded rotor, so that power losses be minimized during the start. The paper analyzes the energetic aspects at the rheostatic startup of the existing three-phase induction motors with wounded rotor, used in conveyor belts actuation, characterized by hard starting. The higher moment of inertia of the system significantly increases the startup time, so it results a higher power consumption and a higher operating cost. A startup improvement can be made, in terms of investment and operating costs, using the main constructive sizes and the electromagnetic data sheet requirements of the induction motor. The study was made on customer request, which proposes a modernization of the start by using an electronically controlled rheostat at the rotor and a three-phase bridge. The paper makes a technical and an economical comparison between the known classic rheostatic starting and the version proposed by the beneficiary. Presented simulations aimed the electricity losses analysis for the wounded rotor induction motors startup. The proposed modernization of the induction motor with wounded rotor that exists at the conveyor, means a controlled starting with lower current shocks, but it results an increased electricity consumption by 10.7% during the start.

***Keywords*—** high power induction motors, startup optimizing.

I. Introduction

THE basic components in all power systems are the electrical machines.

Therefore, the progress in cutting-edge industries is conditioned by developments in electrical machines, so by their performance.

T. C. Author is with the Electrical Engineering Department, University of Colorado, Boulder, CO 80309 USA, on leave from the National Research Institute for Metals, Tsukuba, Japan (e-mail: author@nrim.go.jp).

Ion Vlad is with the University of Craiova, corresponding author; Romania, e-mail: ivlad@em.ucv.ro.

Sorin Enache is with the University of Craiova, Romania, e-mail: senache@em.ucv.ro.

Monica Adela Enache is with the University of Craiova, Romania, e-mail: menache@em.ucv.ro.

Ionut D. Smarandescu is with the University of Craiova, Romania, email: smarandescu.ionut@yahoo.com

It follows, as a necessity, that high power induction motors to have better operating characteristics, higher specific power, and lower overall dimensions and weight [1-4], [8-9].

These requirements are achieved through optimal designing of the motors, which have high energy efficiency, and through new experimental trials and product quality certification [10-15].

The use of performance/advanced computers in the designing and construction activities for wounded rotor induction motors, has restricted the simplifying assumptions, and therefore, numerical mathematical models with a higher number of variables can be used.

Designers should lay down in a short time an optimal asynchronous motor variant that meets the customer's requirements, such as the producing company to gain marketplace and the investment to be effective [4], [6], [16-22].

In this study it is carried out an energetic analysis of the starting regime of the induction motors with wounded rotor of high powers, used in driving systems with large inertia moment.

II. The Mathematical Model and the Objective Function

Modern computers enabled the use of complex numerical mathematical models in the designing stage of the high power wounded rotor induction motors, resulting in superior operating and startup characteristics, respectively reduced production and operating costs.

On a worldwide scale it is imposed an increase in energy efficiency, so that a rational use of electrical energy consumption in industry to be achieved [1-5], [28-30]. This results in a reduction of the operating expenses by minimizing losses of the active and reactive power at load operation and during the induction motors with wounded rotor startup.

A. Objective function

In the paper it is exposed a study of the rheostatic starting (k = 1, 2, ... n steps) for high power induction motors, considering the minimal startup costs criterion [7], [26-27], by using the *objective function*:

$$f(\bar{x}) = C_{ep} = C_{epa} + C_{epr} = \\ = \Sigma T_{pk} (P_{1k\,med} c_{el.a} + Q_{1k\,med} c_{el.r}) \quad (1)$$

where: C_{ep} – total startup cost, C_{epa}, C_{epr} – active and reactive electricity costs at startup, T_{pk} – operating time at step k of the

resistance, $P_{1k.med}$, $Q_{1k.med}$ – the average values of active and reactive power when running on step k, $c_{el.a}$, $c_{el.r}$ – the cost of a kWh for the active or reactive electricity.

The restrictive conditions are those for current limitation during startup: $I_{pmin=} 0{,}9*I_{2N}$ – the lower limit and $I_{pmax} =1{,}2*I_{2N}$ – the upper limit. This limitation determines a sufficient starting torque, even at full load. This provides a lower dynamic torque in order to have a slow, longtime start of the conveyor belt, characterized by a high moment of inertia.

B. Rheostatic starting

In order to reduce the voltage between slip rings to an acceptable value, U_{e20}=2745 V, that doesn't pierce the insulation, the designer opted for the Delta connection at the rotor's winding. Because it is a high power induction motor with wounded rotor, was made a rheostatic starting for limiting the inrush current from the power network [3], [8], [18].

Fig.1.a depicts the Delta connection of the rotor's winding (with the additional resistance on phase included) connected in short-circuit during startup.

Knowing the total resistance for a phase of the rotor - $R_{\Delta p}$ (Fig. 1.a), and r_2 - own resistance for a phase of the rotor, one computed the additional resistance $R_{f\Delta p}$ mounted on a phase at Delta connection:

$$R_{f\Delta p} = R_{\Delta p} - r_2 \tag{2}$$

In Fig.1.b is depicted the switching from Delta to Star connection, and was made using the relationship:

$$R_{yp} = \frac{R_{\Delta p}}{3} = \frac{r_2 + R_{f\Delta p}}{3} = \frac{r_2}{3} + \frac{R_{f\Delta p}}{3} \tag{3}$$

In Fig.1.c is highlighted the rotor's phase resistance $R_{2y}=r_2/3$, supposing it was in Star connection and assuming the conservation condition of the engine operating mode.

In this case, for the additional startup resistance in Star connection, results the value:

$$R_p = \frac{R_{f\Delta p}}{3} \tag{4}$$

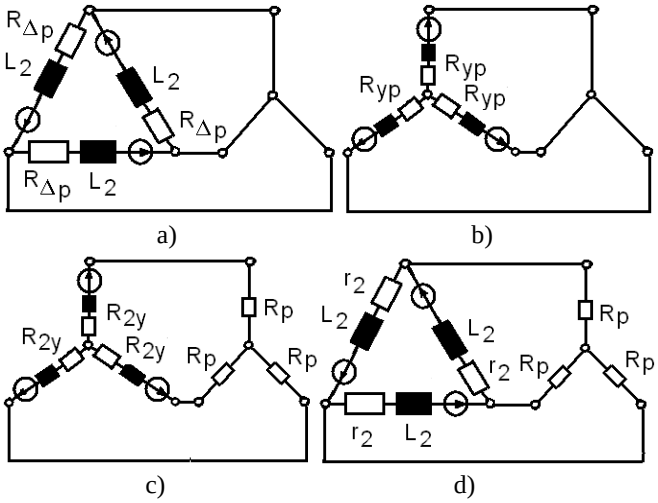

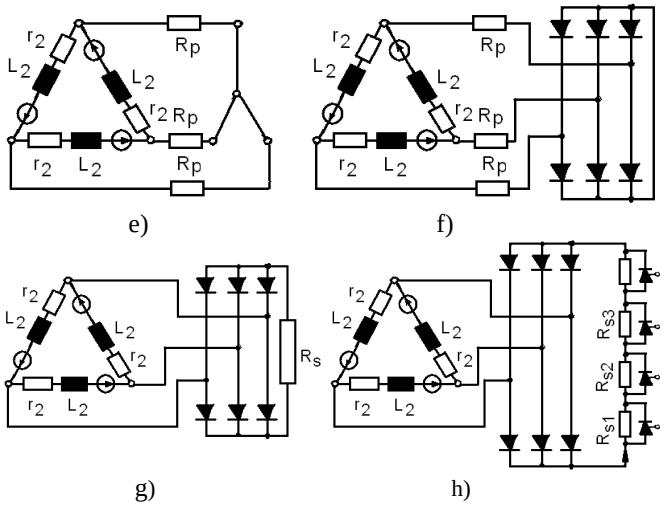

Fig. 1. Connections and necessary transformations to calculate the starting rheostat: a) initial connection where we have the additional resistance; b) the transition from delta to star connection; c) and d) setting the phase resistance at startup R_p; e) and f) transition from star connection to the diode bridge; g) and h) resistance transfer from one phase to the diode bridge.

The rotor passes from Star to Delta connection (Fig.1.d, …, Fig.1.h), and the receiver is kept in Star connection. With the known transformation relations, results the value:

$$r_2 = 3 \cdot r_{2y} = 3 \cdot \frac{r_2}{3} = r_2 \tag{5}$$

namely own known resistance.

It follows from the results that the total resistance of a rotor's phase $R_{\Delta p}$ is determined according to the literature, and then the receptor's phase resistance R_p in Star connection is determined using (4).

III. Results and Simulations

In the paper are analyzed some aspects regarding the startup optimization of the high power induction motors with wounded rotor, the rheostat sizing, the calculation of energy losses.

Analysis was done on a specific case of a high power and high voltage three-phase induction motor with wounded rotor, used to drive long lengths conveyors.

The rated data of the engine are: P_N=3800 kW – rated power, U_N=6 kV – rated voltage, I_{1N}=410 A, I_{2N}= 1330 A, n_1=1000 rot/min – synchronism speed.

The cost for a rheostatic starting of the engine was made for $c_{el.a}$ =0.132 €/kWh - cost of an active electricity kWh, $c_{el.r}$ =0.036 €/kVARh - cost of a reactive electricity kVARh.

A redesign of the engine (according to the literature) gave the following results: $\cos\varphi_m$=0.92; η_m=0.9665; Σp_m=127.3 kW; $M_{max.m}=2.60*M_N$; r_1= 0.043 Ω, r_2= 0.014 Ω, X_1= 0.762 Ω, X_2= 0.27 Ω, k_r=3.621 – reference factor.

A. Analysis of the classical rheostatic startup method

The phase current for the rotor [3], [11] is determined by the relationship:

$$I_{2pk} = \frac{s_k U_{e20}}{\sqrt{\left(R_{\Delta p}\right)^2 + \left(s_k X_2\right)^2}} \quad (6)$$

Using (6), the condition $I_{2pk} = I_{pmax}$ and the slipping s_k, corresponding to the transition on the following step of the resistance, it gives the total phase resistance of the rotor $R_{\Delta pk}$. From the condition $I_{2pk} = I_{pmin}$, equation (6) and resistance value $R_{\Delta pk}$, results the slipping s_k, when switching on the next step. In this way the resistance steps of the starting rheostat are calculated.

For the current limits imposed by the beneficiary, I_{pmin}, I_{pmax}, resulted a starting rheostat with 14 steps, the related features being depicted in Fig.2.

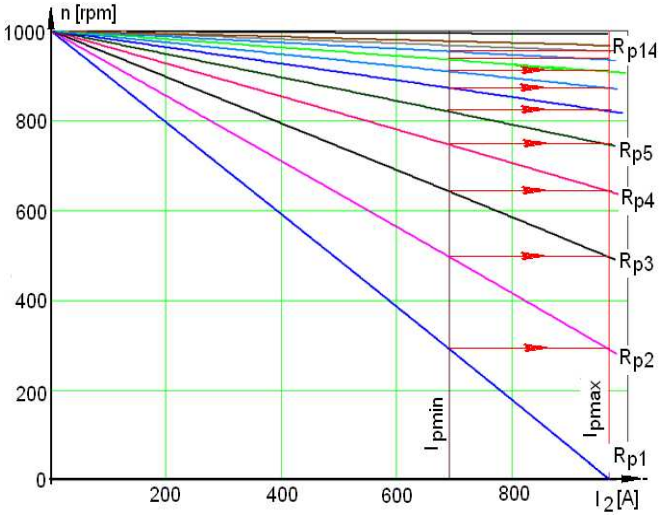

Fig. 2. Rheostatic characteristics necessary for the calculation of the startup rheostat: I_{pmin} and I_{pmax} – limits imposed to the rotor's current.

Further, based on the diagram in Fig.3, a detailed study was been made to highlight the startup's specific measurements. It will be noted $R_{pk}=R_k+R_{k+1}+ \dots +R_{14}$ - the phase resistance, corresponding to the startup on step *k* of the rheostat.

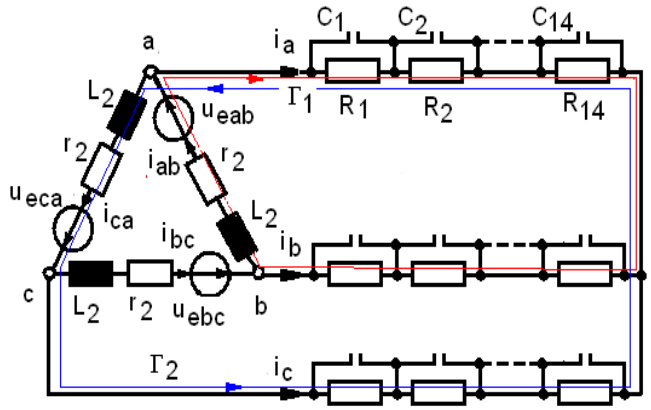

Fig.3. The three-phase electrical scheme of the rotor, the startup step rheostat, and necessary contactors.

The rotor voltages for all three phases have sinusoidal waveforms, as:

$$u_{eab} = \sqrt{2} \cdot s_k U_{e20} \sin(\omega t - 0)$$
$$u_{ebc} = \sqrt{2} \cdot s_k U_{e20} \sin(\omega t - \frac{2\pi}{3}) \quad (7)$$
$$u_{eca} = \sqrt{2} \cdot s_k U_{e20} \sin(\omega t - \frac{4\pi}{3})$$

The equations that describe the motor operation on step *k* of the rheostat, are:

$$r_2 i_{ab} + L_2 \frac{di_{ab}}{dt} + R_{pk} i_a - R_{pk} i_b = u_{eab}$$
$$r_2 i_{bc} + L_2 \frac{di_{bc}}{dt} + R_{pk} i_b - R_{pk} i_c = u_{ebc}$$
$$r_2 i_{ca} + L_2 \frac{di_{ca}}{dt} + R_{pk} i_c - R_{pk} i_a = u_{eca} \quad (8)$$
$$i_{ab} - i_{ca} - i_a = 0$$
$$i_{bc} - i_{ab} - i_b = 0$$
$$i_{ca} - i_{bc} - i_c = 0$$

and from these relationships results:

$$f_{ab}(u_{eab}, i_{ab}, i_a, i_b) = \frac{u_{eab} - r_2 i_{ab} - R_{pk} i_a + R_{pk} i_b}{L_2}$$
$$f_{bc}(u_{ebc}, i_{bc}, i_b, i_c) = \frac{u_{ebc} - r_2 i_{bc} - R_{pk} i_b + R_{pk} i_c}{L_2} \quad (9)$$
$$f_{ca}(u_{cab}, i_{ca}, i_c, i_a) = \frac{u_{eca} - r_2 i_{ca} - R_{pk} i_c + R_{pk} i_a}{L_2}$$
$$i_{ab} - i_{ca} - i_a = 0$$
$$i_{bc} - i_{ab} - i_b = 0$$
$$i_{ca} - i_{bc} - i_c = 0$$

Using these functions and the 4th order Runge Kutta method, it results the numerical solution of the problem (the time variation waveforms of the phase and line currents).

It will be examined the initial startup time n=0, (step k=1, s_k=1), U_{e20}=1730 V – the phase emf with the rotor immovable, r_2= 0.014 Ω, L_2= 0.859 mH – phase resistance and phase inductance for the rotor.

For current limitation imposed condition $I_{2.p} < I_{pmax}=1.2*I_{2N}=1596$ A, results the total phase resistance of the rotor $R_{p1}=R_1+R_2+ \dots +R_{14}$ = 1.75 Ω, (fig.2 and Fig.3).

For the above given values, the equations system (8) is solved and, at the startup moment, the raported phase current wave form is obtained ($i_{ab}=I_{ab}/I_{2fN}$, Fig. 4).

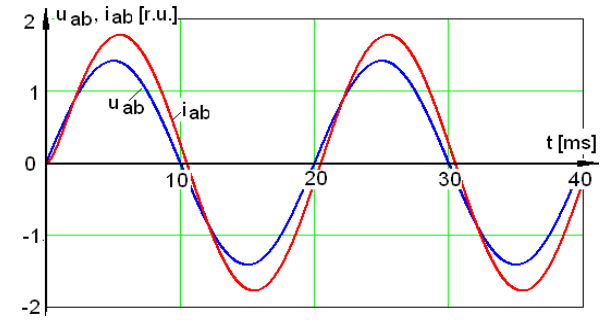

Fig. 4. Time variation curves/waveforms for the phase voltage and current for the phase ab, at classical rheostatic startup.

The effective values of the phase and line currents, respectively, determined by simulation are: I_{abp}= 965 A, respectively I_{ap}= 1671 A.

B. Analysis of the startup for the proposed method

Fig. 4 depicts the modernization solution proposed by the beneficiary, where the rotor's phase resistances are replaced with a single electronically controlled resistance (Fig.5), placed at the exit of the rectifier bridge, putting the condition to preserve the value of the line current in the rotor.

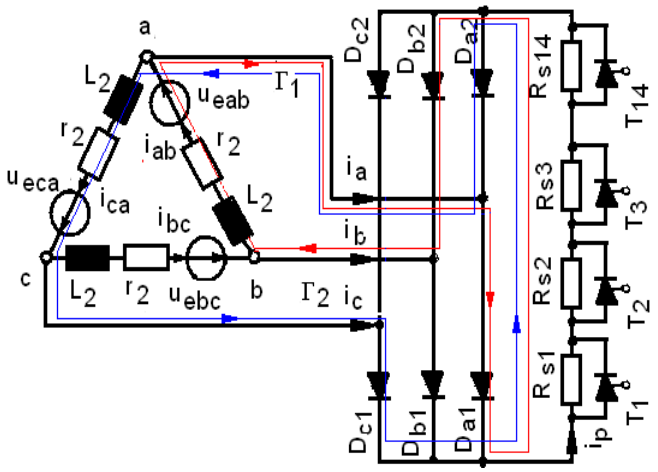

Fig. 5. The three-phase electrical scheme of the rotor, the double bridge, the starting step rheostat and the necessary thyristors.

It will be noted with $R_{ppk}=R_{sk}+R_{sk+1}+ \dots +R_{s14}$ – the load resistance of the rectifier bridge, corresponding to the starting resistance with step *k*. The resulting emf, u_{dab}, for the closed circuit containing the rotor's phase *ab* (Fig. 6), when the diodes D_{a1}, D_{b2} respectively D_{a2}, D_{b1} are conducting, is:

$$u_{d\,ab}=\begin{cases}0 & \omega t=(0\div 60^o)\\ u_{ab} & \omega t=(60^o\div 120^o)\\ 0 & \omega t=(120^o\div 180^o)\\ 0 & \omega t=(180^o\div 240^o)\\ u_{ab} & \omega t=(240^o\div 300^o)\\ 0 & \omega t=(300^o\div 360^o)\end{cases} \quad (10)$$

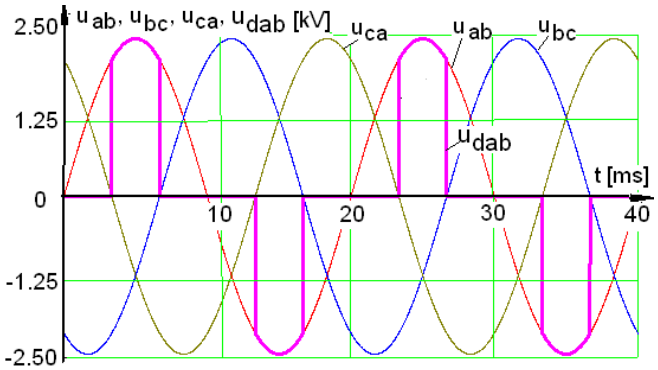

Fig. 6. The induced electromotive voltages on the three phases u_{ab}, u_{bc}, u_{ca} and the resultant voltage u_{dab} for the phase ab.

The equations that describe the motor's operation at step *k* of the rheostat are obtained from (8), where the phase voltages u_{ab}, u_{bc}, u_{ca} are switching with the voltages that occur at the operation of the diode bridge u_{dab}, u_{dbc}, u_{dca}:

$$\begin{aligned}&r_2 i_{ab}+L_2\frac{di_{ab}}{dt}+R_{ppk}i_a=u_{dab}\\ &r_2 i_{bc}+L_2\frac{di_{bc}}{dt}+R_{ppk}i_b=u_{dbc}\\ &r_2 i_{ca}+L_2\frac{di_{ca}}{dt}+R_{ppk}i_c=u_{dca}\\ &i_{ab}-i_{ca}-i_a=0\\ &i_{bc}-i_{ab}-i_b=0\\ &i_{ca}-i_{bc}-i_c=0\end{aligned} \quad (11)$$

The following functions result:

$$\begin{aligned}&f_{ab}(u_{dab},i_{ab},i_a,i_b)=\frac{u_{dab}-r_2 i_{ab}-R_{ppk}i_a}{L_2}\\ &f_{bc}(u_{dbc},i_{bc},i_b,i_c)=\frac{u_{debc}-r_2 i_{bc}-R_{ppk}i_b}{L_2}\\ &f_{ca}(u_{dca},i_{ca},i_c,i_a)=\frac{u_{dca}-r_2 i_{ca}-R_{ppk}i_c}{L_2}\\ &i_{ab}-i_{ca}-i_a=0\\ &i_{bc}-i_{ab}-i_b=0\\ &i_{ca}-i_{bc}-i_c=0\end{aligned} \quad (12)$$

B1. The initial moment of the startup

In order to make a fair comparison with the rheostatic startup classical method, it will be analyzed the same starting time n = 0, (step k=1, s_k=1). To comply with the current limitation imposed condition $I_{2.p}< I_{pmax}=1.2*I_{2N}$, results the total resistance of the diode bridge $R_{pp1}=Rs_1+Rs_2+ \dots +Rs_{14}$ = 0.89 Ω (Fig. 5).

By solving the differential equations system with the 4th order Runge Kutta method, the numerical solution is obtained and results the time variation waveforms for the phase and line currents. Through numerical methods also, are determined the effective value of the phase current I_{ab}=960 A, the fundamental harmonic value I_{ab1}=916 A, the distortion factor k_{dis}= 30.1% and the harmonic spectrum.

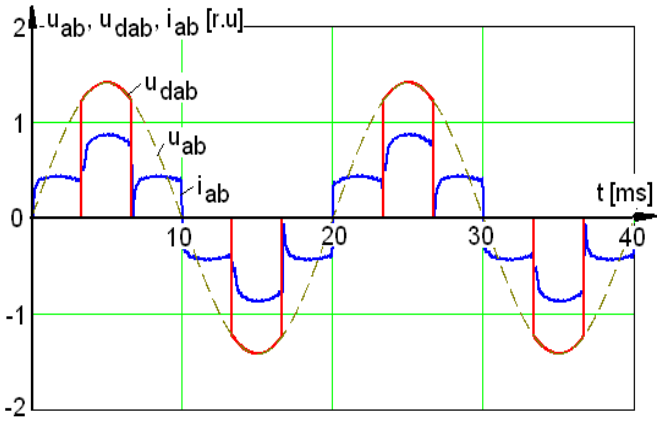

a)

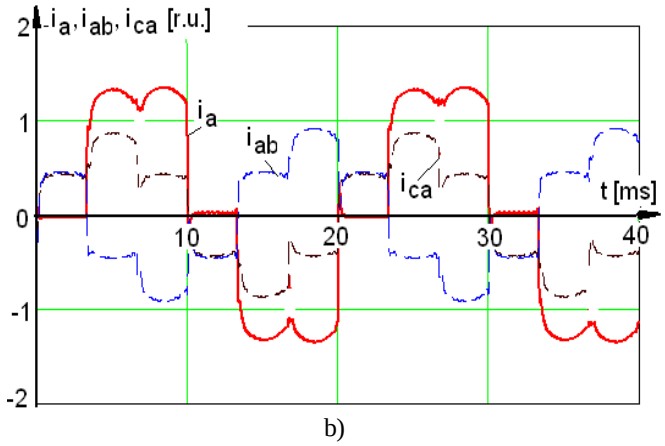

b)

Fig. 7. Time variation curves/waveforms for: a) line voltage, the voltage when the bridge diodes are conducting, b) phase and line currents.

The effective value of the line current is I_a=1670 A, and for the rectified current it results I_{red}=4318 A. . Fig. 7.a depicts the phase voltage and the phase current u_{ab}, i_{ab}, and Fig. 7.b. presents the phase currents i_{ab}, i_{ca} and the resultant line current i_a.

The version proposed by the beneficiary presents a high deformed regime with a rich harmonic spectrum (Fig. 8). In this case, the rotor's fundamental harmonic currents form a symmetrical three-phase system, and ensure the smooth running of the engine. In Fig. 8, the line voltages and currents for all three phases, the rectified current (by the starting resistance), all in relative units, are depicted.

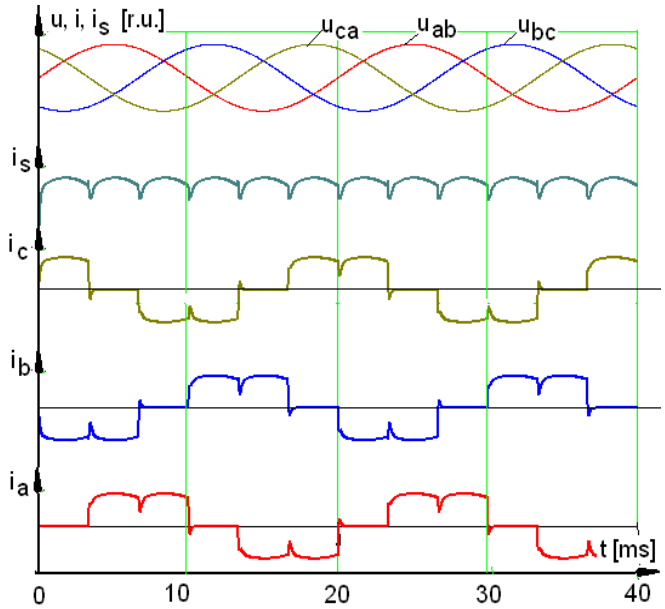

Fig. 8. Time variation curves/waveforms for the analyzed rotoric values: u_{ab}, u_{bc}, u_{ca} – phase voltages; i_a, i_b, i_c – rotor's line currents; i_s – starting resistance current.

B2. Moment when crossing the natural mechanical characteristic

The entrance on the natural mechanical characteristic is made at the speed of n_{14} = 991 r.p.m., s_{14} = 0.0085, therefore, the additional rotor resistance is null R_{ppk}=R_{pp14}= 0 Ω. With this specific values, the system (11) is solved and the numerical solution is obtained (time variation curves/waveforms for the phase and line currents, Fig. 10, the resultant voltages determined by the presence of the diode bridge, Fig. 9).

The phase rms current I_{ab} = 1101 A, fundamental harmonic value I_{ab1} = 948 A, distortion factor k_{dis}= 50.7%, harmonic spectrum, line current I_a= 1666 A, and the rectified current I_{red}= 4324 A.

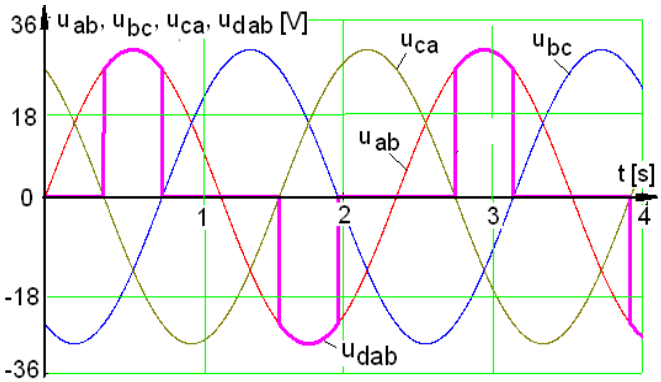

Fig. 9. The induced electromotive voltages on all three phases u_{ab}, u_{bc}, u_{ca} and the resultant voltage u_{dab} on the phase ab.

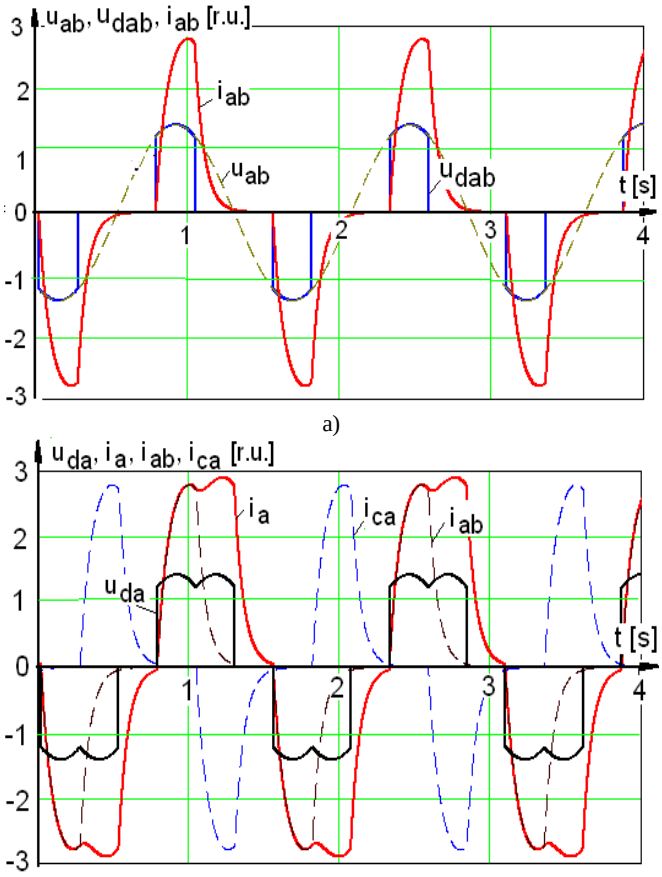

Fig. 10. Time variation curves/waveforms for: a) the line voltage, the resultant voltage, phase ab current; b) the resultant voltage, the phase currents i_{ab}, i_{ca}, and the line current i_a.

For the line currents the time variation/waveform (Fig. 10.b) and the rms values are kept. The phase currents (Fig. 10.a) appear less deformed, with lower peaks and lower harmonic content (Fig.12).

In Fig. 11, the line voltages and currents for all three phases, and the rectified current (through the starting resistance) are depicted, all in relative units.

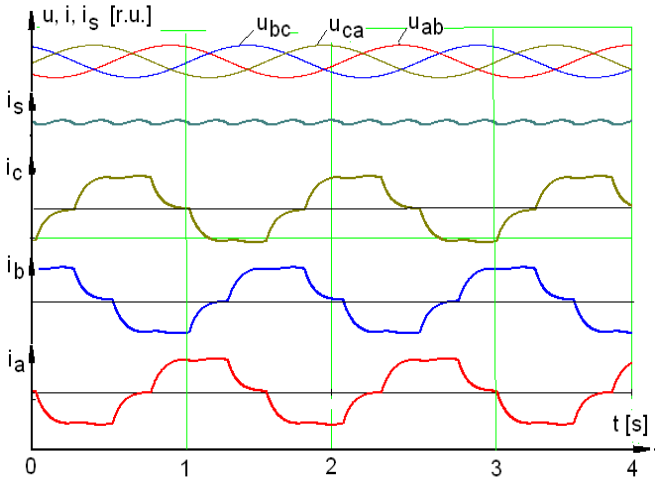

Fig. 11. Time variation curves/waveforms for the analyzed rotoric values: u_{ab}, u_{bc}, u_{ca} – phase voltages; i_a, i_b, i_c – line currents; i_s –the rectified current.

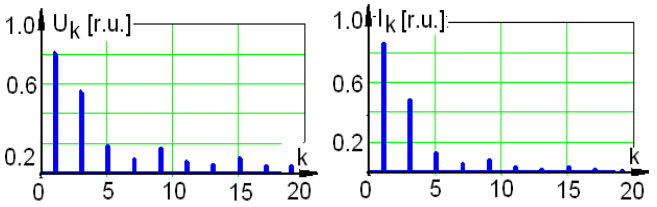

Fig. 12. Harmonic spectrum: a) for the voltage u_{dab}; b) for the phase current i_{ab}.

C. Energy balance at startup

It will be analyzed, in terms of energy efficiency, the starting rheostatic methods (the classical rheostatic starting, and the one proposed by the beneficiary).

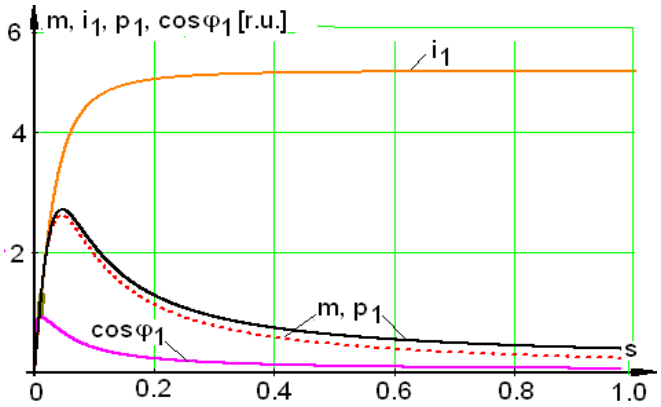

Fig.13. Starting characteristics for direct on-line starting: p_1 –input power, m –torque, i_1 –supply network current, $\cos\varphi_1$ –power factor.

Using the rated data and the motor parameters, for a direct on-line starting, by simulation, there have been established the specific characteristics (current, torque, power factor, input power Fig.13).

Since the conveyor belt has a high moment of inertia, results a lasting startup with a high consumption of electricity.

For the graphic representations depicted in Fig.14 there have been used the relations by literature, and there has been detailed the motor operation on the resistance steps k=1, k=2 and k=14. The rheostat presence ensures a high and almost constant power factor at starting.

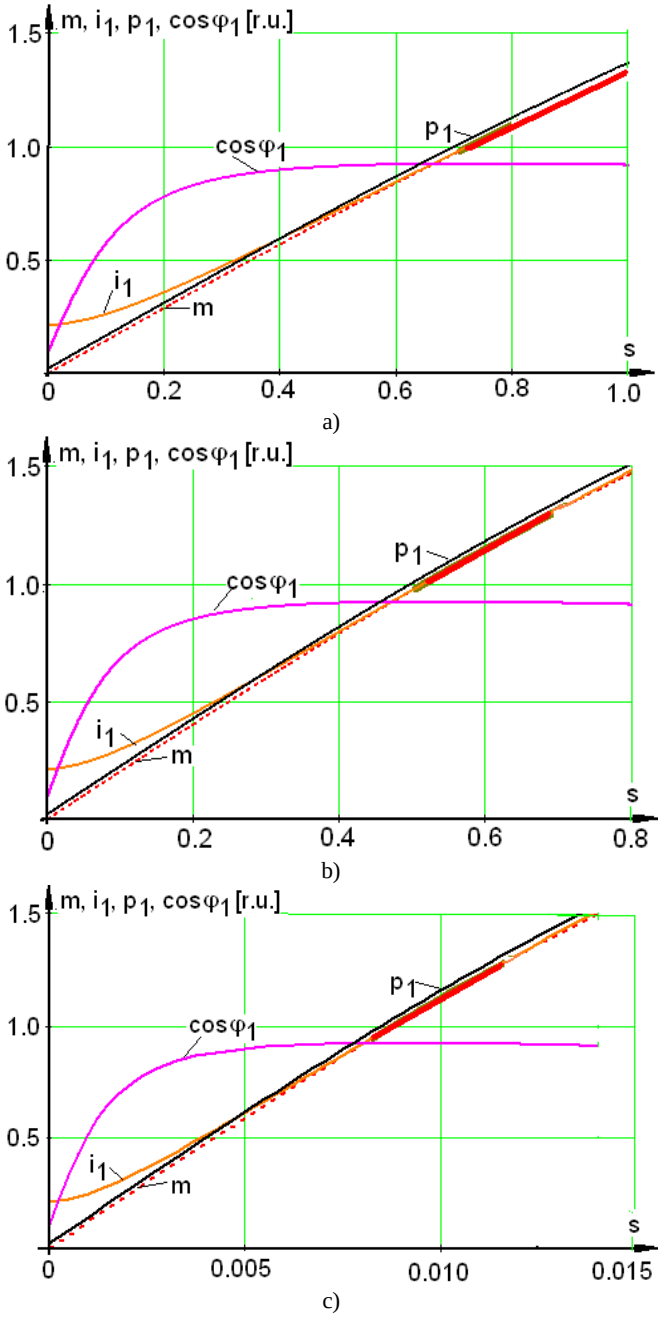

Fig.14. Motor characteristics: p_1 –input power, m –torque, i_1 –supply network current, $\cos\varphi_1$ –power factor for operation on the steps of resistance k=1, k=2 and k=14.

C1. Energy balance at the rheostatic startup

In this case all sizes are sinusoidal and a detailed analysis can be made for the motor operation on each step of the starting rheostat R_{pk} (k=1, 2, 3, ... 14), using the variable s=(0÷1) and the relationships:

$$P_{1_k}(s) = \sqrt{3}U_N I_{1_k} \cos\varphi_{1_k} \quad (13)$$

determined according to the literature [3], [10-11] for the variable s=(0÷1).

At the rheostatic starting the rotor current must be within the limits I_{pmin} =0.9*I_{2N} = 1197 A and I_{pmax} = 1.2*I_{2N}= 1596 A. When it reaches the minimum value of the current, is given the command to close the contactor C_i (Fig.2), corresponding to the operation step.

For the step resistance R_{pk} and the imposed limits (I_{pmax}, I_{pmin}) results the proper slidings s_{k-1} si s_k, respectively the speeds n_{k-1}, n_k. Using the motion equation, the relationship is obtained which allows us to calculate the operating time on the step resistance R_{pk}, having the speed as variable.

$$Tp_k = \sum_{i=n_{k-1}}^{n_k} \frac{2\pi J_t}{M_k(s_i) - M_r}(n_i - n_{i-1}) \quad (14)$$

The total duration of the startup will be:

$$Tp = \sum_{k=1}^{14} Tp_k \quad (15)$$

The average value of the active power from the grid when running on step R_{pk} is:

$$P_{1k\,med} = \sum_{i=s_{k-1}}^{s_k} \frac{P_{1k}(s)}{N} \quad (16)$$

N - is the number of points of the range (s_{k-1},….s_k).

The energy costs during start up will be:

$$C_p = \sum_{k=1}^{14} P_{1kmed} Tp_k c_{el.a} \quad (17)$$

C2. Energy balance at the proposed rheostatic startup

Because we have a deformed regime during startup, for the proposed rheostatic starting method, all determinations are made through numerical methods by using the previous relationships.

In Fig.15 we have the rotor winding in Delta connection, the three-phase rectifier bridge, the 14 resistances used at startup and the thyristors that take out of circuit the step resistances.

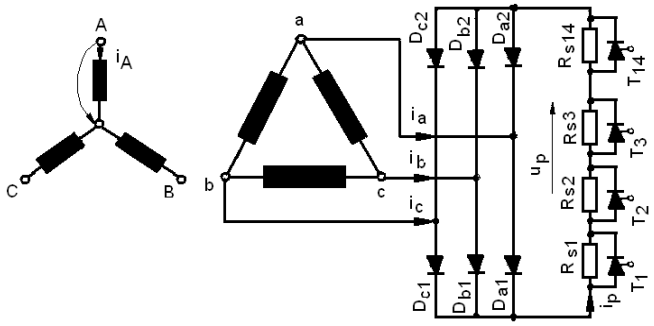

Fig.15. Scheme proposed for starting with resistance of the asynchronous motor.

During the operation at step resistance R_{ppk}, with corresponding slides s_{k-1} and s_k (and speeds n_{k-1}, n_k), the powers P_{1k} are determined by numerical calculation using the relationships by literature. The results obtained for the two methods of starting with resistance we analyzed are filled in the table no. 1.

Table no.1

Starting step (k)	Classical method with resistance				Proposed method with resistance			
	R_{pk} (Ω)	P_{kmed} (MW)	T_k (s)	C_p (E)	R_{pk} (Ω)	P_{kmed} (MW)	T_k (s)	C_p (E)
1	0.583	4.537	13.94	2.319	0.890	4.546	15.358	2.560
2	0.414	4.533	9.998	1.662	0.632	4.542	11.030	1.837
3	0.292	4.531	7.124	1.184	0.446	4.540	7.864	1.309
	…	…	…	…	…	…	…	…
14	0.000	4.503	0.193	0.043	0.000	4.533	0.297	0.051
Total			48.47	8.081			53.621	8.946

IV. Experimental Results in Laboratory on Model

There are carried out laboratory experiments with a low power wound rotor three-phase asynchronous motor, for verifying the validity of the proposed mathematical model.

The results experimentally obtained during the starting period are compared to the simulations carried out for this motor.

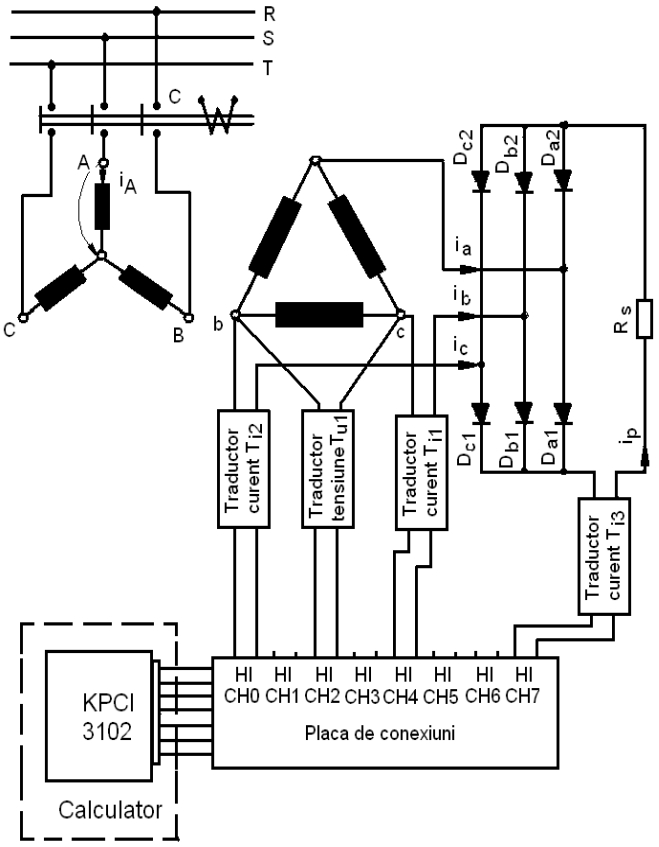

Fig.16. Scheme and devices necessary for determining the quantities for starting with resistance.

In the scheme depicted in Fig.16 we have: M.A.-wound rotor three-phase asynchronous motor, KPCI 3102-system for

acquiring and processing experimental data, C –contactor, R_p – starting rheostat. The rated data of the motor are: P_N= 4 kW, U_N= 380 V, I_{1N}=9.18 A, I_{2N}= 18.5 A, n_1=1000 r.p.m., cosφ= 0.78, η= 0.85. By re-designing the motor the following quantities have been obtained: $M_{max.m}$=2.37*M_N; r_1=1.041 Ω, r_2= 0.722 Ω, X_1= 2.129 Ω, X_2= 1.25 Ω, k_r=1.44 – reference factor.

Using the mathematical model given by (11), the reference data of this motor and a resistance R_p=R_{ppk}= 14 Ω (from the condition of limiting the current $I_{2.p}$< 1.2*I_{2N}), there have been carried out simulations for starting.

Using the system for acquiring, processing and measuring electrical quantities, it is possible to see the curves of voltages and line currents for no-load starting with resistance for the three-phase asynchronous motor from the laboratory (the rotor was blocked).

In Fig.17 there has been plotted the curve of the rotor current simulation for starting, nesinusoidal quantity. The curve of the experimental line current and the harmonic spectrum are depicted in Fig.18, THD=22%, and the phase current in Fig.19. We notice a high distortion factor THD=26.2%, for the two currents (a rich harmonic spectrum), that means high starting losses.

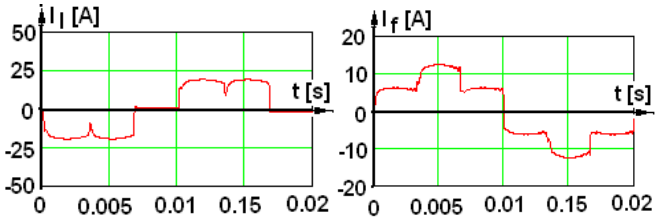

a) b)

Fig. 17. Currents curves obtained by simulation in the starting moment for an asynchronous motor rated at P_N=4 kW: a) line, b) phase.

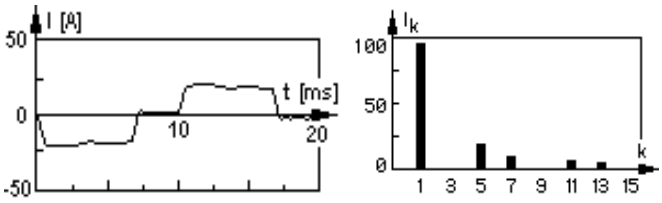

a) b)

Fig. 18. Curve recorded for the rotor line current (fig. a), and the harmonic spectrum (fig.b).

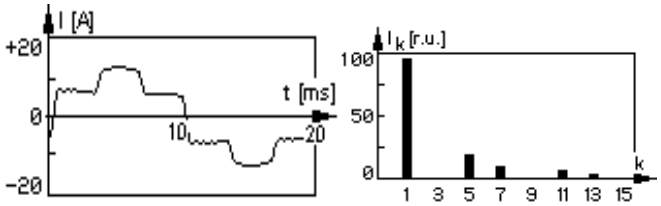

a) b)

Fig. 19. Curve recorded for the phase rotor current (fig. a), and the harmonic spectrum (fig.b).

From the comparison between the results obtained by simulation and the experimental results, it results:

-the quantitative differences between the real curves and the simulated ones are small and they occur owing to the magnetic saturation which modifies the machine inductances.

V. Conclusions

The study performed on customer's demand, aimed to compare functionally and energetically the two methods of rheostatic starting (classical with three-phase rheostat and the proposed method with single-phase electronically controlled rheostat).

As investment, for the classical starting a three-phase rheostat with 14 steps is used; it must stand the current I_p=1670 A. The method we proposed uses a single-phase rheostat with 14 electronically controlled, but of current I_{pp}=4318 A. Consequently, the rheostat volume and the cost are the same for the two cases.

In terms of energy, the classical rheostatic startup means a lower cost of energy consumption by 10.7% and a reduced process time by 10.6%.

The solution proposed by the beneficiary, with the single-phase electronically controlled rheostat, means a reduction in the amount of the fundamental harmonic for a imposed value of the rotor current. This explains the increased startup time and increased energy consumtion for the new method.

Taking into account the problem of reducing the energetic consumption in exploitation is a very present one, the study we carried out for high power asynchronous motors is justified.

References

[1] M. Ancau, L. Nistor, Tehnici numerice de optimizare în proiectarea asistată de calculator, Bucuresti, Ed. Tehnică, 1996.

[2] M. Biriescu, V. Cretu, M. Mot, "Testing of Electrical Machines Using a Data Acquisition and Processing System", Workshop on Electrical Machines' Parameters, Cluj Napoca, Romania, May 2001.

[3] A. Boukhelifa, M. Kherbouch, A. Cheriti, R. Ibtiouen, O. Touhami, R. Tahmi, "Stator current minimization by field optimization in induction machine", International Conference on Electrical, Electronic and Computer Engineering, ICEEC'04, 2004.

[4] B.K. Bose, "Power Electronics and Motor Drives Recent Progress and Perspective", Industrial Electronics, IEEE Transaction on Volume 56, Issue: 2, 2009, pp.581-588.

[5] C.U. Brunner, "International Standards for Electric Motors", Standards for Energy Efficiency of Electric Motor Systems (SEEEM), 2007, pp. 6-10.

[6] A. Campeanu, A. Ionescu, I. Vlad, S. Enache, "Prediction through simulation of the optimal behavior of the induction machine in complex process", SPEEDAM 2008, Ischia, pp. 1136-1140.

[7] A. Campeanu, I. Vlad, S. Enache, L. Augustinov, G. Liuba, I. Cautil, "Optimization of startup characteristics of medium power asynchronous motors with short circuit rotor", ICEM'2012, Marseille.

[8] M. Centner, U. Schäfer, "Machine design software for induction machines," in Proc. ICEM, Vilamoura, Portugal, 2008, pp. 1–4.

[9] J. Faiz, M.B.B. Sharifian, "Optimal design of three-phase Induction Motors and their comparison with a typical industrial motor", Computers and Electrical Engineering, vol. 27, 2001, pp. 133-144.

[10] I. Daniel, I. Munteanu,s.a., Metode numerice in ingineria electrica. Bucuresti, Editura Matrix Rom, 1998.

[11] Q. Hecker, W. Meyer, P. Bahr, H. Herzog, "Development and Algorithmic Implemetation of a new Concept for the Preliminary draft of Electrical Machines", ICEM 2012, pp.1276-1281.

[12] J. Hofmann, "Innovative Motor Design for Production Machines", Electric Drives Production Conference (EDPC) 2011, pp.198-201.

[13] J.D. Kueck, D.A. Casada, P.J. Otaduy, “A comparison of two Energy Efficient Motors”, IEEE Transactions on Energy Conversion, vol.13, nr.2, iunie, 1998, pp.140-147.
[14] O. Muravlev, et al, “Energetic parameters of induction Motors as the basis of energy saving in a variable speed drive, ” Electrical Power Quality and Utilization, Vol. IX, No. 2, 2005.
[15] M. Mihai, A. Simion, L. Livadaru, A. Munteanu, “Induction Motor with Switchable Number of Poles and Toroidal Winding”, AECE Journal, Vol.11, Issue 2, Year 2011, pp.113-118.
[16] M. Sames, "Optimization of induction motor design", Zeszyty Naukowe Politechniki Slaskiej Seria Elektryka, z. 176, 2001, pp.103-110.
[17] D. Samarkanov, F. Gillon, P. Brochet, D. Laloy, “Interval arithmetic tool for Optimal Design of Induction Machines”, ICEM 2012, pp.1346-1351.
[18] D. Samarkanov, F. Gillon, P. Brochet, D. Laloy, “Techno-economic Optimization of Induction Machines: an Industrial Application”, ACEMP - Electromotion 2011, Istanbul –Turkey, 8-10 September 2011, pp. 825-830.
[19] A. Simion, L. Livadaru, S. Mihai, A. Munteanu, C.G. Cantemir, “Induction Machine with Improved Operating Performances for Electric Trucks. A FEM-Based Analysis”, AECE Journal, Vol.10, Issue 2, Year 2010, pp.71-76.
[20] G.A. Soares, A.S. Pedroso, “Induction motor optimization design: A contribution for energy efficiency program”, ICEM-1998, pag. 1500-1503.
[21] V.M. Stanciu, M. Cistelecan, V. Nitigus, M. Popescu, "Politics for the use of electric machines with high electric efficiency", Electrical Engineering, Electronics and Automation Journal, Vol. 53, no. 3, 2005, Bucharest, Romania.
[22] A. Taheri, A. Rahmati, S. Kaboli, “Energy Optimization of Field Oriented Six-Phase Induction Motor Drive”, AECE Journal, Vol.11, Issue 2, Year 2011, pp.107-112.
[23] H. Toliat, “Recent Advances and Applications of Power Electronics and Motor Drives-Electric Machines and Motor Drives”, Proc. of IECON, 2008.
[24] T. Tudorache, M. Popescu, “Optimal Design Solutions for Permanent Magnet Synchronous Machines”, AECE Journal, Vol.11, Issue 4, Year 2011, pp.77-82.
[25] T. Tudorache, L. Melcescu, “FEM Optimal Design of Energy Efficient Induction Machines”, AECE Journal, Vol.9, Issue 2, Year 2009, pp.58-64.
[26] I. Vlad, A. Campeanu, S. Enache, Monica Enache, “Aspects regarding optimal design of high power squirrel cage asynchronous motors”, OPTIM 2012, pp. 503 – 508.
[27] I. Vlad, A. Campeanu, S. Enache, Monica Enache, “Aspects regarding design of squirrel cage asynchronous motors for mining excavators”, Anals of the University of Craiova, Series Electrical Engineering, Year 36, No. 36, 2012, pp. 57-62.
[28] I. Vlad, A. Campeanu, S. Enache, Proiectare asistată a maşinilor asincrone. Probleme de optimizare, Craiova, Editura Universitaria Craiova, 2011.
[29] A.Yazidi, H. Henao, G. Capolino, F. Betin, F. Fillipetti, “A Web-Based Remote Laboratory for Monitoring and Diagnosis of AC Electrical Machines”, Industrial Electronics, IEEE Transaction on Volume 58, Issue: 58, 2011, pp.4950-4959.
[30] *** CEI 60034-2-1 Standard: "Rotating electrical machines-Part 2-1. Standard methods for determining losses and efficiency from tests", Edition 1.0, 2007.